Chemical Engineering Journal 165 (2010) 465–473

Contents lists available at ScienceDirect

Chemical Engineering Journal

journal homepage: www.elsevier.com/locate/cej

Cr(III) ionic imprinted polyvinyl alcohol/sodium alginate (PVA/SA) porous composite membranes for selective adsorption of Cr(III) ions

Jian Hua Chen[a,*], Guo Ping Li[a], Qing Lin Liu[b], Jian Cong Ni[a], Wen Bing Wu[a], Jin Mei Lin[a]

[a] Department of Chemistry and Environmental Science, Zhang zhou Normal University, Zhangzhou 363000, China
[b] Department of Chemical and Biochemical Engineering College of Chemistry & Chemical Engineering, Xiamen University, Xiamen 361005, China

ARTICLE INFO

Article history:
Received 2 July 2010
Received in revised form
23 September 2010
Accepted 24 September 2010

Keywords:
Sodium alginate
Membrane
Polyvinyl alcohol
Adsorption
Cr(III)

ABSTRACT

In the present study, we prepared Cr(III) ionic imprinted membrane adsorbents (Cr(III)-PVA/SA) by blending sodium alginate (SA) with polyvinyl alcohol (PVA). In these new membrane adsorbents, polyethylene glycol was used as porogen, and glutaraldehyde was the cross-linking agent. Our new developed membrane adsorbents can be used without centrifugation and filtration. To investigate the adsorption kinetics of Cr(III) ions from aqueous solution onto this newly developed Cr(III)-PVA/SA, we performed a batch of experiments under different conditions by changing the concentration of Cr(III) ions in the Cr(III)-PVA/SA, pH value of the solution, adsorbent dose, initial Cr(III) ions concentration, adsorption temperature and contact time. Our Cr(III)-PVA/SA exhibited the maximum Cr(III) ions uptake capacity of 59.9 mg/g under the following conditions: 0.078 wt% of Cr(III) ions in the Cr(III)-PVA/SA, solution pH value of 6.0, adsorbent dose of 0.5 g/L, the initial Cr(III) ions concentration of 50 mg/L, at 25 °C. To study the mechanism of adsorption process, we examined the intra-particular diffusion model, Lagergren pseudo-first-order kinetic model and pseudo-second-order kinetic model, and found pseudo-second-order kinetic model exhibited the best correlation with our experimental data. Furthermore, our adsorption equilibrium data could be better described by the Langmuir equation. Competitive adsorption studies of the binary system of Cr(III)/Cu(II), Cr(III)/Cd(II) and the ternary system of Cr(III)/Cu(II)/Cd(II) were also investigated using Cr(III)-PVA/SA, the results indicated that selectively adsorbed amount of Cr(III) ion on Cr(III)-PVA/SA is significantly higher than that of Cu(II) and Cd(II) ions. We also used five times consecutive adsorption–desorption experiments to show that the Cr(III)-PVA/SA has high adsorption and desorption efficiencies.

1. Introduction

With the rapid increase in global industrial activities, heavy metal pollution has become more serious. The discharge of toxic and polluting heavy metal ions into the environment by the mining operations, metallurgical, electroplating, battery manufacturing, nuclear and other industries is posing serious risk to the environment [1,2]. Treatment for high volumes of wastewater containing low concentrations of heavy metals pollutants is becoming increasingly important as the discharge regulations become more stringent. One of the major toxic metal ions endangering human life is chromium. Cr(III) ions compounds are widely used in modern industries, such as leather making, metal finishing and petroleum refining, which inevitably results in a large quantity of Cr(III) ions contaminated industrial effluents. Waters containing a high concentration of Cr(III) ions are extremely harmful to human beings because they are non-biodegradable in living tissues and would induce toxic and carcinogenic health effects on humans [3–5]. Therefore, the technology for effective removal of Cr(III) from water and wastewater is urgently needed.

Over the past decades, a number of technologies have been developed to remove heavy metal ions from aqueous solutions, such as adsorption, co-precipitation, ion exchange, chemical reduction and membrane separation [6–17]. Removal of Cr(III) ions from wastewater by adsorption has been investigated by many researchers. The main advantages of the adsorption are recovery of the heavy metal, high selectivity, less sludge volume produced, simplicity of design and the meeting of strict discharge specification. Also, it has been a strong alternative to other processes because of its ability to reduce dissolved chromate concentration to none detectable levels in the water treatment plants.

One of the recently developed techniques for the preparation of highly effective adsorbent is the ion-selective imprinting technique, where the specific recognition capability is provided to the host molecules by addition and subsequent extraction of template molecules/ions [18–20]. Molecular imprinting is a

* Corresponding author. Tel.: +86 596 2591445; fax: +86 596 2520035.
E-mail address: jhchen73@126.com (J.H. Chen).

1385-8947/$ – see front matter © 2010 Elsevier B.V. All rights reserved.
doi:10.1016/j.cej.2010.09.034

promising technique for preparing polymeric materials with artificial receptor-like binding sites for various substances, and the molecular imprinted materials for its recognition function has been utilized in many fields, such as solid-phase extractions, membrane separations and sensors [21–24]. Recently, the heavy metal ions imprinting adsorbent, for its excellent selective separation performance for trace heavy metals, has became more concerned.

In recent years, increased attention has been focused on the use of naturally available low cost biomaterials for removing heavy metal ions from wastewater [25,26]. Compared to other traditional treatment processes, heavy metal adsorption using biomaterials can reduce total capital cost greatly. Use of biomaterials also even makes the adsorption process more environmental friendly and more technically feasible. SA is naturally occurring polysaccharides obtained mainly from marine brownalgae belonging to the Phaeophyceae, composed of two monomeric units, h-D-mannuronic acid and a-L-guluronic acid [27]. SA, for its good membrane forming properties and high activity with carbonyl and hydrogen groups on its chain, has been attracted considerable attention currently.

The objective of this present work is to explore the potential utilizing of Cr(III) ionic imprinted Cr(III)-PVA/SA for adsorption removal of Cr(III) ions contaminated from wastewater. To investigate the effects of operating factors on the adsorption capacity of the Cr(III)-PVA/SA for Cr(III) ions, We carried out a batch of adsorption experiments under different conditions by varying the concentration of Cr(III) ions in the Cr(III)-PVA/SA, pH value of the solution, adsorbent dose, initial Cr(III) ions concentration of the solution, adsorption temperature, and contact time. By testing various adsorption and kinetics models to fit our experiment data, we also studied the adsorption kinetics and isotherms of Cr(III) ions adsorption for the Cr(III)-PVA/SA. The competitive adsorption of Cr(III)-PVA/SA for Cr(III) ions from binary heavy metal mixed system and ternary heavy metal mixed system were examined, and the desorption and reusability of the Cr(III)-PVA/SA for adsorption Cr(III) ions were also investigated.

2. Experimental

2.1. Materials and analytical method

All the chemicals and reagents used were of analytical grade and obtained from Sinopharm Chemical Reagent Co. Ltd. A stock solution of 100 mg/L of Cr(III) ions was prepared by dissolving 1.5420 g of $Cr(NO_3)_3{\cdot}9H_2O$ in 2000 mL distilled water. This solution was diluted as required. A series of standard Cr(III) ions solution were prepared by appropriate dilution of the stock Cr(III) ions solution. Solutions of 0.1 M NaOH or HCl were used for pH adjustment. The concentration of Cr(III) ions in the samples was determined from the linear calibration curve.

2.2. Preparation of Cr(III) ionic imprinted Cr(III)-PVA/SA composite membranes

1 g of PVA, 1 g of SA and 0.06 g of polyethylene glycol(PEG) were dissolved in deionized water and stirred at 90 °C for 90 min, then the hot solution were filtered. This was followed by the addition of various amount of $Cr(NO_3)_3{\cdot}9H_2O$ (Cr^{3+} account for 0.026, 0.52, 0.067, 0,078, 0.091 and 0.104 wt% based on the total amount of PVA, SA and PEG) solution drop by drop with continuous stirring. Then, 5 wt% GA (2.0 mL) and 1.0 M HCl (2.0 mL) were added into the above solution and stirred vigorously for 60 min. The resulting solution was cast on a glass plate, and then dried in an oven at 70 °C for 120 min. The dried membranes were subsequently peeled off and immersed into deionized water for one day to remove the porogen PEG. Finally, the obtained membranes were immersed into 0.1 M HCl for 60 min to remove the imprinted Cr(III) ions, then immersed into deionized water again for one day. The resulted membranes were dried in an oven at 100 °C for 120 min, then, stored in a desiccator for further experiment.

2.3. Membrane characterization

FT-IR spectra of the Cr(III)-PVA/SA before and after Cr(III) ions adsorption were scanned in the range from 4000 to 400 cm^{-1} with an accumulation of 16 scans on a Nicolet-740. The surface morphology of the Cr(III)-PVA/SA before and after adsorption were also characterized by using SEM (LEO 1530, Oxford Instruments), equipped with the energy dispersive X-ray spectroscope, which was operated at EHT = 20 kV.

2.4. Adsorption procedure

The stock Cr(III) ions solution with concentration of 100 mg/L was prepared by using $Cr(NO_3)_3{\cdot}9H_2O$ as a source of Cr(III) ions. Experimental solutions of the desired concentrations were obtained by successive dilution. The pH of the solution was maintained at desired value by adding 0.1 M HCl or NaOH solution before adsorption experiment. Adsorption experiments were carried out in a 500 mL volumetric flask using 250 mL Cr(III) ions solution with required amount of adsorbent. The flasks were placed on an orbital shaker running at 120 rpm at 25 ± 1 °C until equilibrium was reached. 5 mL of the sample was drawn at regular intervals for residual concentration testing. The chromium equilibrium concentration was spectrophotometrically measured using standard procedure at λ = 420 nm [28]. All the experiments were performed in triplicate and the average of three was taken for subsequent calculations. The difference between duplicate experimental values was in the range of ±1.5%.

The adsorption capacity of the Cr(III)-PVA/SA was evaluated by using the following expression:

$$q_t = \frac{(C_0 - C_t)V}{m} \quad (1)$$

where q_t is the amount of Cr(III) ions adsorbed on unit mass of the adsorbent PVA/SA (mg/g), C_0 and C_t are the concentration of the Cr(III) ions in the initial solution and in aqueous phase after adsorption for a t min (mg/L); V is the volume of the aqueous phase (L); and m is the amount of adsorbent Cr(III)-PVA/SA used (g), respectively.

2.5. Selectivity adsorption experiments

0.125 g of Cr(III) ionic imprinted Cr(III)-PVA/SA was added to a 250 mL of Cr(III)/Cd(II), Cr(III)/Cu(II) binary mixed solutions and Cr(III)/Cd(II)/Cu(II) ternary mixed solution (initial concentration of single species 50 mg/L), respectively; then, the pH value of the solution was adjusted to 6.0 by adding certain amount of 0.1 M HCl; finally, the flasks were placed on an orbital shaker running at 120 rpm at 25 ± 1 °C until equilibrium was reached. The concentration of Cr(III), Cd(II) and Cu(II) in the solutions were spectrophotometrically measured.

2.6. Desorption of heavy metal ions and membrane reusability

Desorption of heavy metal ions was achieved using 0.1 M HCl as a desorbing agent. The metal loaded Cr(III)-PVA/SA membrane samples were placed in the 250 mL desorption medium at 25 °C, with a shaking speed of 120 rpm for 120 min. The membrane samples were washed with a deionized water several times and subjected again to adsorption/desorption process for five cycles.

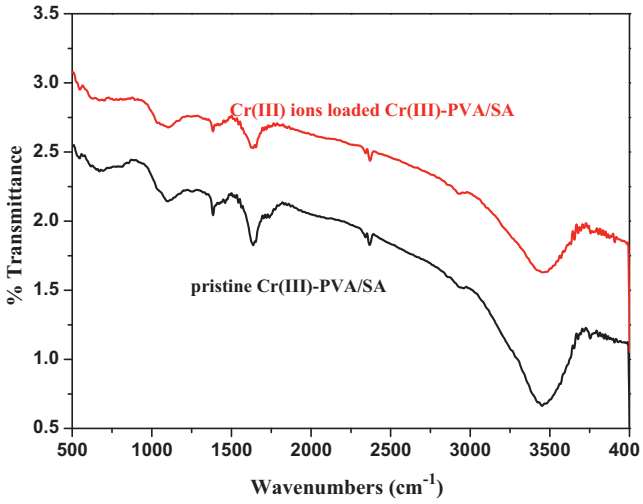

Fig. 1. FT-IR spectra of Cr(III)-PVA/SA before and after adsorption.

3. Results and discussion

3.1. Characterization of Cr(III)-PVA/SA

3.1.1. FT-IR analysis

The FT-IR spectra of the Cr(III)-PVA/SA before and after Cr(III) ions adsorption are presented in Fig. 1. A strong and broad band appeared around 3447.64 cm^{-1} corresponding to O–H stretching vibrations, while the band at 1633.52 cm^{-1} might be due to C=O stretching of carbonyl group. Comparing the FT-IR spectra of the Cr(III)-PVA/SA before and after Cr(III) ions adsorption, we can find that the characteristic bands mentioned above of the latter are slightly affected in their position and intensity. It indicates that the adsorption of Cr(III) ions on the surface of Cr(III)-PVA/SA is either through complexation or through physical way which might be through weak electrostatic interaction and Vander Waals forces [29]. However no chemical bonding takes place in this process. The FT-IR spectra of Cr(III) ions loaded Cr(III)-PVA/SA shows elongation of these bands after Cr(III) ions adsorption indicating the role of these group in adsorption.

3.1.2. SEM images

The SEM images of the Cr(III)-PVA/SA before and after Cr(III) ions adsorption are shown in Fig. 2. The SEM images clearly shown that the reaction of Cr(III) ions with Cr(III)-PVA/SA made the surface of Cr(III) ions loaded Cr(III)-PVA/SA less rough and protrusions. In order to further investigation the surface characteristic of the Cr(III)-PVA/SA before and after Cr(III) ions adsorption, we also performed an energy dispersive X-ray (EDX) analysis. The results are shown in Fig. 3(a and b). From Fig. 3(a), we found that it did not show the characteristic signal of Cr(III), which, however, was clearly observed in the Fig. 3(b).

3.2. Effects of the concentration of template Cr(III) ions on adsorption

To investigate the effects of the concentration of template Cr(III) ions on the Cr(III)-PVA/SA adsorption for Cr(III) ions, we carried out the adsorption experiments at adsorbent dose of 0.5 g/L, solution pH value of 6.0, initial Cr(III) ions concentration of 50 mg/L, and at 25 °C. It can be found from Fig. 4 that the saturated adsorption amount initially increased with higher concentration of Cr(III) ions, and the reason for this is that the amount of imprinted cavities in Cr(III)-PVA/SA are enhanced when the number of Cr(III) ions

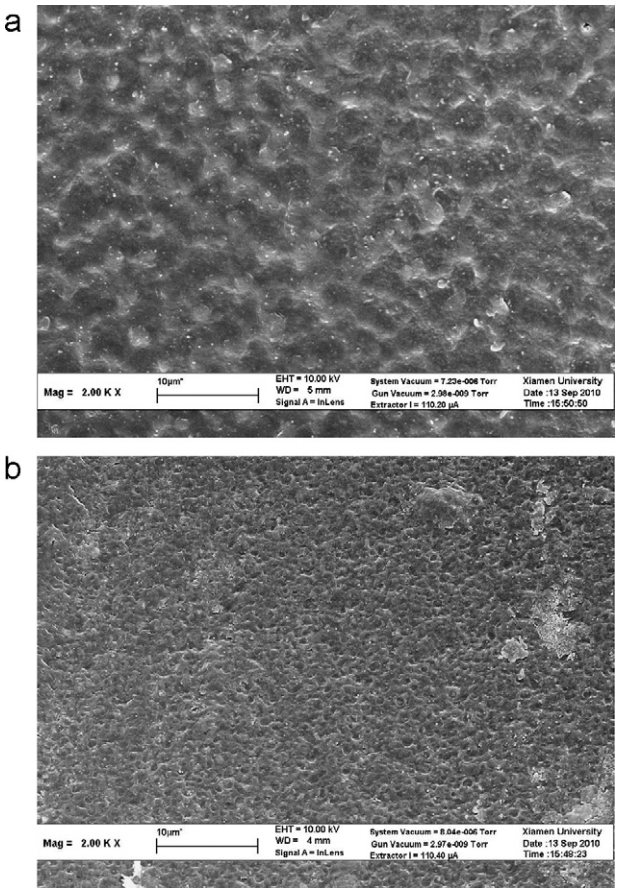

Fig. 2. SEM images of Cr(III)-PVA/SA: (a) before adsorption and (b) after adsorption.

increases, so the saturated adsorption amount of Cr(III)-PVA/SA increase. As the concentration of Cr(III) ions arrives at 0.078 wt%, a turning point appears on the curve, and after this point, the adsorption amount of Cr(III)-PVA/SA decreases slightly. This result indicates that under the condition of the concentration of Cr(III) ions arrives at 0.078 wt%, a maximum concentration of imprinted cavities have been formed during imprinting, so the number of imprinted cavities decreases slightly even if the concentration of Cr(III) ions further increases. Therefore, the Cr(III)-PVA/SA with Cr(III) ions concentration of 0.078 wt% was used for further adsorption experiments.

3.3. Effects of pH value of the solution on adsorption

pH value of the solution is an important controlling parameter that strongly affects the adsorption behavior of the adsorbent for heavy metal ions. In order to optimize the pH value for maximum removal efficiency, we performed the adsorption experiments under the following condition: pH values of the solution in the range of 2.0–10.0, adsorbent dose of 0.5 g/L, initial Cr(III) ions concentration of 50 mg/L, and at 25 °C. From Fig. 5, we found that pH value of the solution significantly affected the adsorption of Cr(III)-PVA/SA for Cr(III) ions. Adsorption capacity q_e reached maximum at the pH value of 6.0 and decreased at lower or higher pH values. This behavior can be explained by the change in the ionic state of the acid functional carboxyl groups in the adsorbent [30,31]. At pH value of the solution lower than the pK_a, functional groups were protonated, and Cr(III) ions uptake capacity decreased. Meanwhile, chromic ion species exist in acidic solution as bulky hydrated species ($Cr(H_2O)_6^{3+}$), this ion was too large to enter in the micro-porous of the Cr(III)-PVA/SA [32,33].

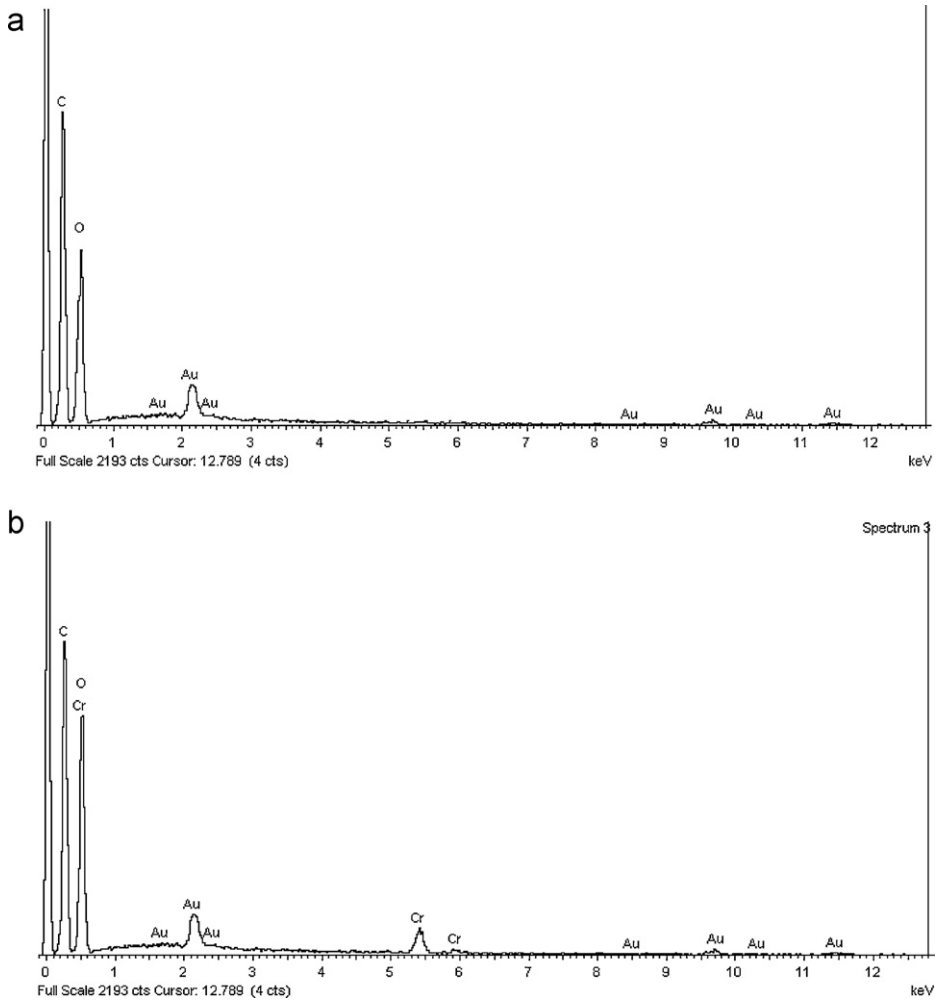

Fig. 3. Energy dispersive X-ray (EDX) analysis of Cr(III)-PVA/SA: (a) before adsorption and (b) after adsorption.

At pH value higher than the pK_a, carboxyl groups were negatively charged and Cr^{3+} ion (principal species at low pH value) can be bound to negative charged groups by electrostatic attraction. A further increasing in pH value results in a decreasing of Cr^{3+} concentration and other species become important, such as $CrOH^{2+}$ and monovalent $Cr(OH)_2^+$, which diminished Cr(III) ions adsorption at pH value higher than 6.0. Meanwhile, precipitate could occurred at a higher pH value. To make sure the maximum removal efficiency as well as to avoid precipitation of Cr(III) ions, all the following experiments were conducted at solution pH value of 6.0.

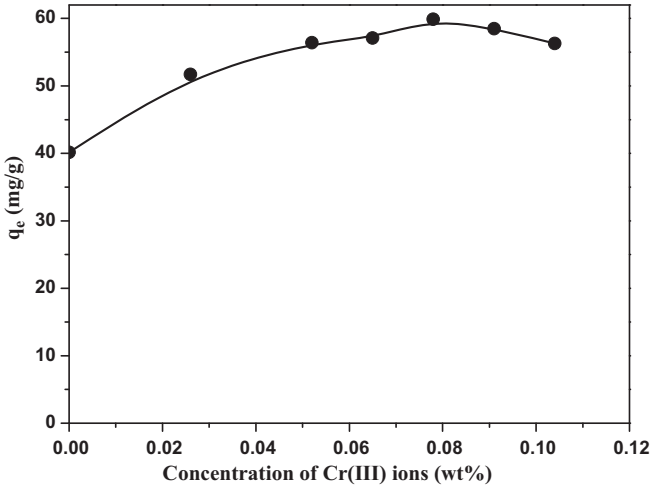

Fig. 4. The effects of the concentration of template Cr(III) ions on adsorption.

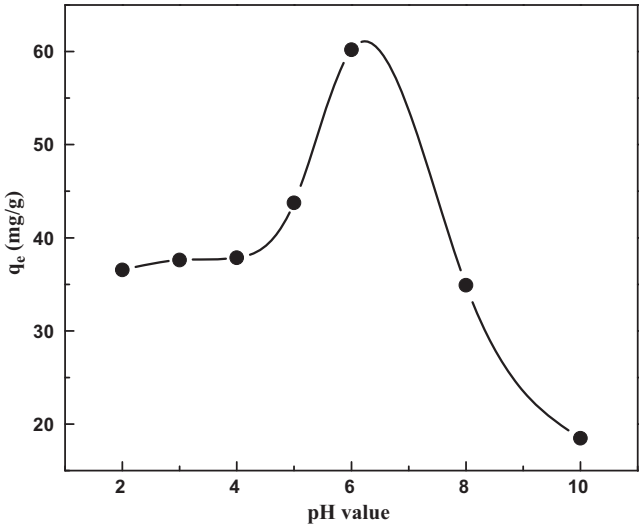

Fig. 5. The effects of pH value of the solution on adsorption.

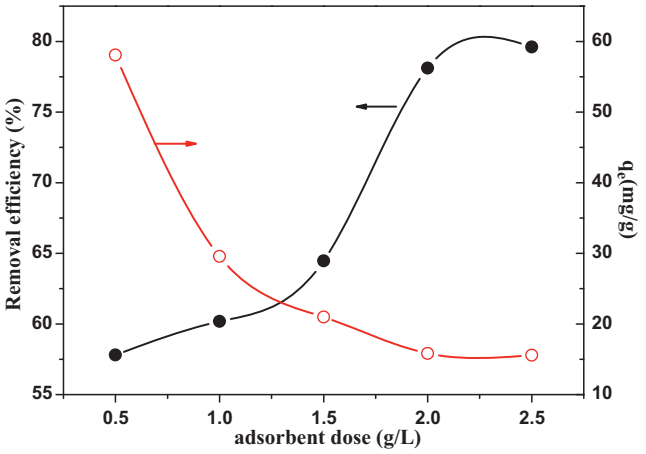

Fig. 6. The effects of adsorbent dose on adsorption.

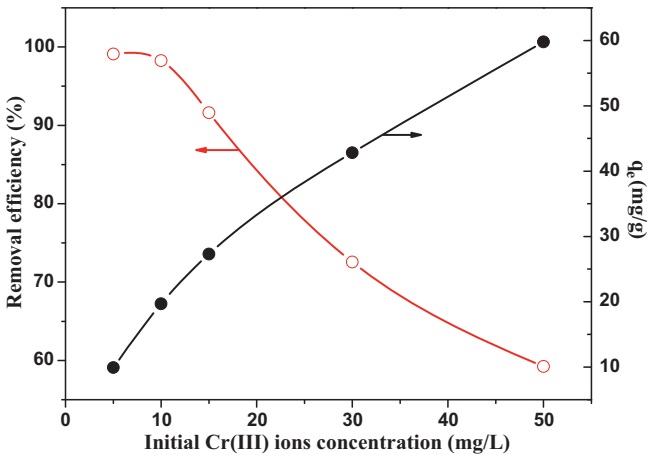

Fig. 7. The effects of initial Cr(III) ions concentration on adsorption.

3.4. Effects of adsorbent dose on adsorption

The adsorbent dose is another important parameter because it has direct relation to the adsorption capacity of an adsorbent for metal ions at a given initial concentration at the operating conditions. To evaluate the effects of adsorbent dose on adsorption behavior, we conducted the experiments with adsorbent dose in the range of 0.5–2.5 g/L, initial Cr(III) ions concentration of 50.0 mg/L, pH value of 6.0, and at 25 °C. Fig. 6 indicated that when the adsorbent dose increased from 0.5 to 2.5 g/L the percentage of Cr(III) ions removal increased from 57.8 to 79.7%, however, the Cr(III) ions uptake capacity of the adsorbent decreased from 59.9 to 15.6 mg/g. From the results, we concluded that Cr(III) ions removal efficiency increased but adsorption density decreased during the increasing of the adsorbent dose. The decrease in adsorption density can be attributed to the fact that some of the adsorption sites remain unsaturated during the adsorption process; whereas the number of available adsorption sites increased with more adsorbent, and this results in better removal efficiency. Furthermore, we also observed that the amount of Cr(III) ions removal attained an asymptotic value for a larger dose of adsorbent after rapid increase in adsorption percentage of Cr(III) ions with an increase in adsorbent dose up to 2.0 g/L. The sluggish rise in Cr(III) ions removal beyond an optimum dose may be attributed to the attainment of equilibrium between adsorbate and adsorbent under the experimental conditions.

3.5. Effects of initial Cr(III) ions concentration on adsorption

In batch adsorption processes, the initial metal ion concentration of the solution plays a key role as a driving force to overcome the mass transfer resistance between the solution and solid phases. Therefore, the amount of metal ions adsorbed was expected to be higher with a higher initial metal ions concentration. The adsorption capacity of Cr(III) ions was investigated in correlation with the variation in the initial Cr(III) ions concentrations in the range of 5.0–50.0 mg/L (pH value of 6.0; adsorbent dose of 0.5 g/L; at 25 °C) and the obtained data were plotted in Fig. 7. We can find that when the initial Cr(III) ions concentration increased from 5.0 to 50.0 mg/L, Cr(III) ions removal ability decreased from 99.1 to 59.8%, however, the Cr(III) ions uptake capacity of the Cr(III)-PVA/SA increased from 9.9 to 59.9 mg/g. This can be explained from three aspects. Firstly, a higher concentration of Cr(III) ions led to more binding sites on the surface of Cr(III)-PVA/SA compared to lower initial Cr(III) ions concentration at the same dose of adsorbent [7]; Secondly, higher initial Cr(III) ions concentration increased driving force to overcome the mass transfer resistance of Cr(III) ions between the aqueous and solid phases resulting in higher probability of collision between the Cr(III) ions and Cr(III)-PVA/SA; Lastly, the increase of Cr(III) ions uptake capacity of the Cr(III)-PVA/SA with increasing initial Cr(III) ions concentration may also be due to a more intensity interaction between the Cr(III) ions and Cr(III)-PVA/SA.

3.6. Effects of temperature on adsorption

It has been recognized that the adsorption of heavy metal ions from an aqueous solution by adsorbent is affected by the temperature. An increasing in temperature is known to increase the diffusion rate of the adsorbate molecules across the external boundary layer and within the pores of the adsorbent. Furthermore, changing the temperature will modify the equilibrium capacity of the adsorbent for a particular adsorbate. To investigate the effects of temperature on the adsorption capacity of the Cr(III)-PVA/SA for Cr(III) ions, we carried out the adsorption experiment under the following condition: adsorbent dose of 0.5 g/L, initial Cr(III) ions concentration of 50.0 mg/L, pH value of 6.0, and temperature in the range of 25–55 °C. From Fig. 8, we found that the adsorption capacity increased slowly with higher temperature. The increase in Cr(III) adsorption capacity of the adsorbent with higher temperature indicated the endothermic nature of the adsorption process in this study. The increase in Cr(III) uptake capacity with the higher

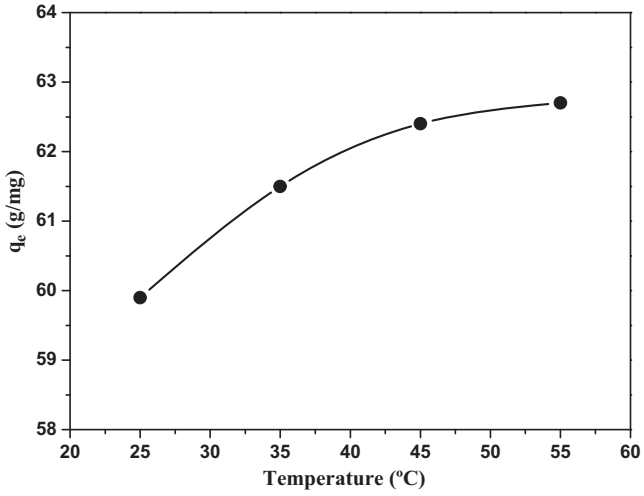

Fig. 8. The effects of temperature on adsorption.

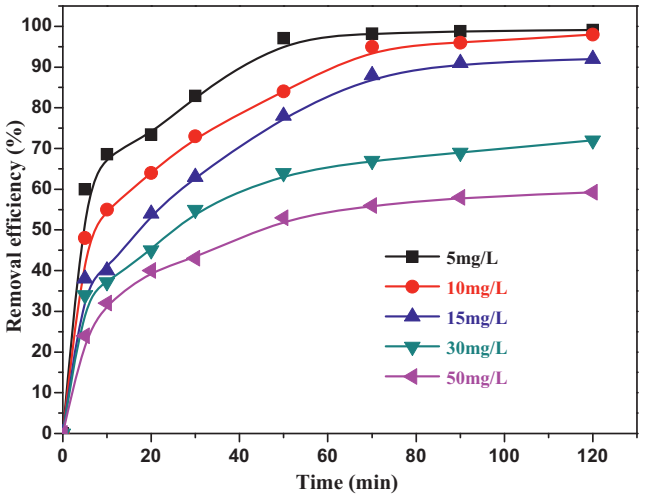

Fig. 9. The effects of contact time on adsorption.

temperature explained from two aspects. Firstly, as the temperature rises, the diffusion of Cr(III) ions becomes much easier into the Cr(III)-PVA/SA because of the increase in the degree of swelling, so the adsorption amount of Cr(III) ions increases as well. Secondly, bond rupture of the functional groups on adsorbent surface at an elevated temperature may increase the number of active adsorption sites, which may also lead to an enhanced adsorption capacity of the adsorbent. We also found that the increase in uptake capacity was not obvious from 25 to 55 °C. Hence, for the convenience and reality, the experiments were carried out at room temperature, which was about 25 °C.

3.7. Adsorption kinetics and isotherms study

3.7.1. Adsorption kinetics study

The adsorption kinetics experiments were carried out at adsorbent dose of 0.5 g/L, Cr(III) ions concentration in the range of 5.0–50.0 mg/L, pH value of 6.0, at 25 °C. The effects of contact time on Cr(III) ions adsorption capacity are presented in Fig. 9. Increase in removal efficiency with increase in time of contact is due to the fact that more time becomes available for Cr(III) ions to interaction with Cr(III)-PVA/SA. It also shows that Cr(III)-PVA/SA is very effective for removal of Cr(III) ions. The Cr(III) ions adsorption is rapid within the first 50 min, then increase slowly, and the adsorption process attained equilibrium within 120 min. Therefore, the adsorption experiments in the following text were conducted for 120 min, except the indicated. The initial Cr(III) ions adsorption rate by Cr(III)-PVA/SA is very high as a large number of adsorption sites are available for adsorption. Meanwhile, in the initial pristine surface, the sticking probability is large and consequently adsorption proceeds with a high rate. Once the available free surface are gradually filled up by the adsorbate species, adsorption process becomes slow and the kinetics may become more dependent on the rate at which the adsorbate molecules penetrate through the pore and get adsorbed on the surface of the inside pores. In order to examine the mechanism of adsorption processes, such as mass transfer and chemical reaction, we tested the Lagergren pseudo-first-order kinetic model and pseudo-second-order kinetic model, the intra-particular diffusion model [12,34,1] with our experiments data.

(1) Lagergren pseudo-first-order kinetic model:

$$\ln(q_e - q_t) = \ln q_e - k_1 t \quad (2)$$

Table 1
Lagergren pseudo-first-order rate parameters for Cr(III) ions adsorption on PVA/SA at 25 °C (adsorbent dose 0.5 g/L, initial Cr(III) ions 5, 10, 15, 30, and 50 mg/L, pH value of 6.0, time 120 min).

Initial Cr(III) ions concentration	q_e (mg/g)	k_1 ($\times 10^{-2}$ min^{-1})	$q_{e,c}$ (mg/g)	R^2
5	9.91	5.42	7.45	0.9409
10	19.60	4.63	15.21	0.9312
15	27.28	4.21	22.43	0.9383
30	42.82	4.04	29.55	0.9346
50	59.71	3.52	47.96	0.9312

Table 2
Lagergren pseudo-second-order rate parameters for Cr(III) ions adsorption on PVA/SA at 25 °C (adsorbent dose 0.5 g/L, initial Cr(III) ions 5, 10, 15, 30, and 50 mg/L, pH value of 6.0, time 120 min).

Initial Cr(III) ions concentration	q_e (mg/g)	k_2 ($\times 10^{-2}$ min^{-1})	$q_{e,c}$ (mg/g)	R^2
5	9.91	5.86	10.67	0.9960
10	19.60	1.23	20.58	0.9920
15	27.28	0.31	29.57	0.9821
30	42.82	0.14	44.43	0.9881
50	59.71	0.05	65.86	0.9841

(2) pseudo-second-order kinetic model:

$$\frac{t}{q_t} = \left(\frac{1}{k_2 q_e^2}\right) + \frac{t}{q_e} \quad (3)$$

where q_e and q_t denote the amounts of adsorption at equilibrium and at time t (mg g^{-1}); k_1 and k_2 are the first order and second order rate constants (min^{-1}), respectively.

The amount of adsorption equilibrium q_e, the rate constants of the equation (l/min), k_1 and k_2, the calculated amount of adsorption equilibrium, $q_{e,c}$, and the coefficient of determination, R^2 were shown in Tables 1 and 2, respectively. Comparing Table 2 with Table 1, we found that the pseudo-second-order equation appears to be the better-fitting model because it has the higher R^2; meanwhile, the calculated amount of adsorption equilibrium ($q_{e,c}$) from pseudo-second-order equation is similar to the actual amount of adsorption equilibrium (q_e).

(3) Intra-particular diffusion model:

$$q_t = k_{dif} t^{1/2} \quad (4)$$

where q_t is the amounts of adsorption at time t (mg g^{-1}), and k_{dif} is the intra-particular diffusion rate constant (mg g^{-1} min$^{-1/2}$). The relation plots of q_t versus time $t^{1/2}$ are shown in Fig. 10. It shows that the plots do not go through origin, which indicates that the adsorption of Cr(III) ions on Cr(III)-PVA/SA is a multistep limited adsorption process.

3.7.2. Adsorption isotherms study

In a two-state system consisting of adsorbent and solution, the adsorption results in the removal of solute from the solution onto adsorbent surface until the remaining solute in the solution is in dynamic equilibrium with solute on the adsorbent surface. A plot of the solute concentration in the adsorbent phase q_e (mg/g) as function of the solute concentration in the solution C_e (mg/L) at equilibrium gives an adsorption isotherm. An adsorption isotherm can be utilized to obtain information about the interaction between the adsorbent and adsorbate molecules. It can also be used to predict the relative performance of different types of adsorbents. In order to understand and clarify the adsorption process, Langmuir adsorption isotherm and Freundlich adsorption isotherm models were applied in this study.

The Langmuir adsorption isotherm equation is the frequently used adsorption model on completely homogenous surface with

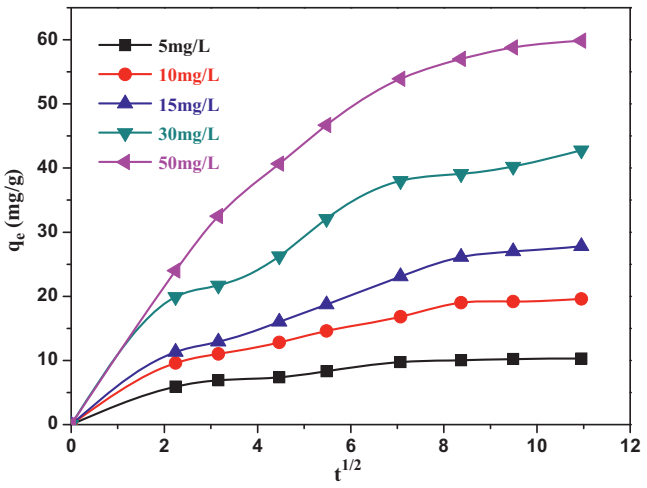

Fig. 10. Investigate intra-particular diffusion model for Cr(III) ions adsorption on the Cr(III) -PVA/SA.

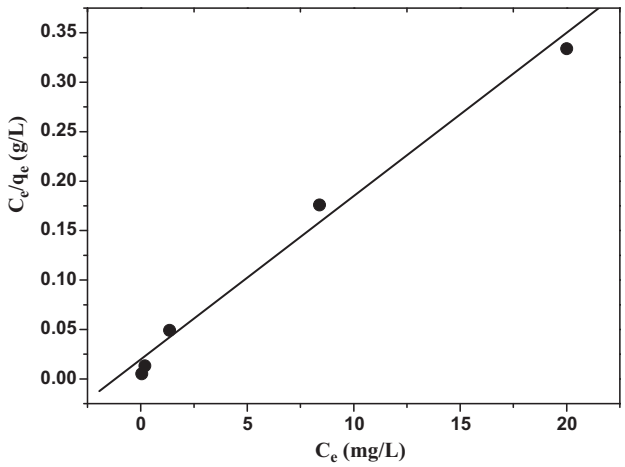

Fig. 11. The Langmuir adsorption isotherm for Cr(III) ions adsorption on Cr(III)-PVA/SA.

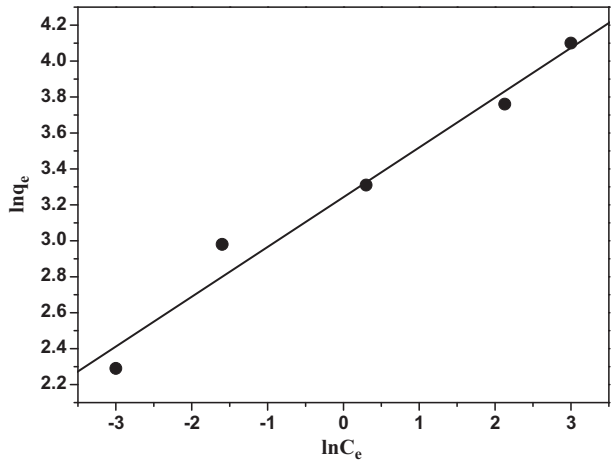

Fig. 12. The Freundlich adsorption isotherm for Cr(III) ions adsorption on Cr(III)-PVA/SA.

negligible interaction between adsorbed molecules, shown as below:

$$\frac{C_e}{q_e} = \frac{1}{bq_{max}} + \frac{C_e}{q_{max}} \quad (5)$$

where q_e is the amounts of adsorption at equilibrium (mg/g), C_e is the equilibrium concentration (mg/L). q_{max} is the adsorption capacity (mg/g), and b is the adsorption intensity or Langmuir coefficient related to the affinity of the binding site (L/mg).

The Freundlich adsorption isotherm equation is an equation based on heterogeneous surfaces suggesting that binding sites are not equivalent and independent, expressed as below:

$$q_e = K_F C_e{}^{1/n} \quad (6)$$

where K_F and $1/n$ are the constants that are related to the adsorption capacity and the adsorption intensity, respectively. The equation can be rewritten in the linear form by taking the logarithm of both sides as following:

$$\ln q_e = \ln K_F + \frac{1}{n} \ln C_e \quad (7)$$

The isotherm constants were calculated from the slope and intercept of Fig. 11 (Langmuir isotherm) and Fig. 12 (Freundlich isotherm) and presented in Table 3. Taken into consideration the values of the correlation coefficient as a criterion for goodness of fit for the system, the Langmuir isotherm model shows better correlation (R^2 = 0.988) than Freundlich isotherm (R^2 = 0.960), which indicated that Langmuir adsorption isotherm model represented the adsorption process more ideally. It suggested the homogeneous nature of the adsorption of Cr(III) ions on Cr(III)-PVA/SA. q_{max} value defined as the maximum capacity of adsorbent calculated from the Langmuir plots is 60.563 mg/g, which agreed closely with the calculation from Lagergren pseudo-second-order equation.

3.8. Competitive adsorption

In order to examine the selective adsorption of ionic-imprinted Cr(III)-PVA/SA for Cr(III) ions, we carried out a competitive adsorption of Cr(III), Cd(II) and Cu(II) from their binary and ternary model mixtures and the results are presented in Table 4. We

Table 3
Langmuir and Freundlich isotherm constants for the Cr(III) ions adsorption at solution pH value of 6.0 and 25 °C.

Adsorbent	Langmuir isotherm parameters			Freundlich isotherm parameters		
	q_{max} (mg/g)	b (L/mg)	R^2	K_F (mg/g)	n	R^2
Cr(III)-PVA/SA	60.563	0.994	0.988	5.127	3.611	0.960

Table 4
Competitive adsorption of Cr(III) ionic imprinting PVA/SA for heavy metal Cr(III), Cd(II) and Cu(II) from the binary and ternary mixed system.

Adsorbent	Cr(III)/Cd(II)		Cr(III)/Cu(II)		Cr(III)/Cd(II)/Cu(II)		
	$q_{e\,Cr(III)}$	$q_{e\,Cd(II)}$	$q_{e\,Cr(III)}$	$q_{e\,Cu(II)}$	$q_{e\,Cr(III)}$	$q_{e\,Cd(II)}$	$q_{e\,Cu(II)}$
Cr(III)-PVA/SA	47.4	10.1	43.2	16.8	39.2	6.8	12.7

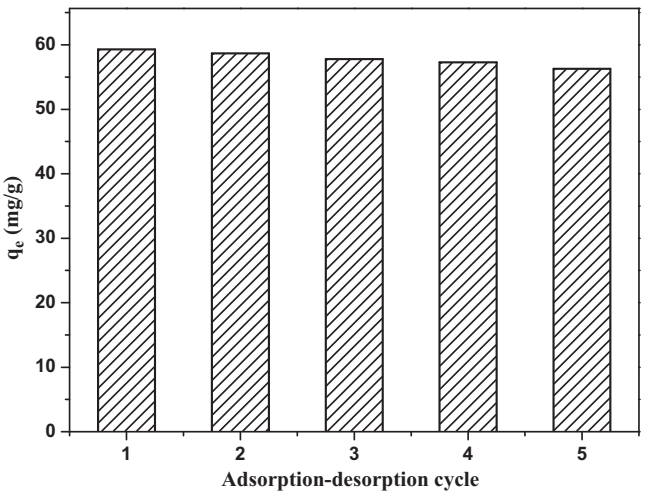

Fig. 13. The reusability of Cr(III)-PVA/SA for removal of Cr(III) ions.

found that the adsorption capacity of the Cr(III)-PVA/SA for Cr(III) ions was much higher than that for Cd(II) and Cu(II) ions. This mainly due to the imprinted cavities existed in the Cr(III)-PVA/SA, which, serve as adsorption sites, suited Cr(III) ions in size and shape.

3.9. Desorption of heavy metal ions and reusability

In order to evaluate the reusability of the adsorbent, we carried out the consecutive adsorption–desorption process for five times using the same adsorbent. Just as Fig. 13 indicated the total adsorption capacity of the Cr(III)-PVA/SA for Cr(III) ions after five cycles decreased slightly from 59.3 mg/g to 56.4 mg/g, no more than 5.0%. The result indicated that the prepared Cr(III)-PVA/SA could be effectively used for treatment wastewater containing Cr(III) ions at least for five times.

Table 5
Adsorption capacity of Cr(III) ions by various adsorbents.

Adsorbent	Maximum adsorption capacity (mg/g)	Reference
Tannin-immobilized mesoporous silica bead	67.6	[3]
Ion-exchange resin	20.28	[5]
Cyphos IL104 functionalized silica sorbents	2.14	[12]
[A336][C272] functionalized silica sorbents	2.32	[12]
Meranti sawdust	16	[29]
Meranti	37.88	[29]
Sawdust grafted poly (methacrylic acid)	36.63	[30]
AFC	30.77	[34]
Vineyard pruning waste	12.45	[35]
Borassus aethiopum	6.24	[36]
Brazilian peats	40.9	[37]
Vermiculite pure clay mineral	46.95	[38]
Alumina adsorbents-functionalized-purpurogallin	29.64	[39]
Lakhra coal	2.61	[40]
Tartrazine modified activated carbon	16.9	[41]
Tris(2-aminoethyl) amine functionalized silica gel	32.72	[42]
Lignin	17.97	[43]
Activated carbon	39.56	[44]
Cr(III) ionic imprinting PVA/SA	59.91	Present work

4. Comparison of uptake capacity of Cr(III)-PVA/SA with other adsorbents'

A comparison of the present maximum uptake capacity with the published results is important to assess the potential application of the Cr(III)-PVA/SA. The present data were compared in Table 5 with the available literature data. From Table 5, we found that the Cr(III) ions uptake capacity of the Cr(III)-PVA/SA was much higher than reported elsewhere, with one exception.

5. Conclusion

In current study, we prepared the novel porous membrane adsorbent Cr(III)-PVA/SA by ionic imprinting technology, which can be efficiently used for adsorption of Cr(III) ions from aqueous solution. Chromium adsorption on the Cr(III)-PVA/SA surface was proved by FT-IR, SEM and EDX methods. The adsorption capacity of the new developed Cr(III)-PVA/SA for Cr(III) ions could reach the maximum (59.9 mg/g) when we kept the adsorption experiment parameters under the optimal condition. The kinetic adsorption data fit well to the pseudo-second-order kinetic model. Meanwhile, the kinetic experiment results also indicated that the rate of controlling step was mainly intra-particle diffusion but was not the only rate-limiting step for Cr(III) ions adsorption. The equilibrium data can be well fitted with the Langmuir adsorption isotherm equation. Competitive adsorption studies for Cr(III)/Cd(II), Cr(III)/Cu(II) binary mixed system and Cr(III)/Cd(II)/Cu(II) ternary mixed system show that Cr(III)-PVA/SA are highly selective to Cr(III) ions due to the imprinted cavity existed in the adsorbent. The consecutive adsorption–desorption experiment shows that the Cr(III)-PVA/SA can be used with high reusability. Hence, we believed that Cr(III)-PVA/SA can be considered as a potential adsorbent for removing Cr(III) ions from the aqueous solution in term of high-effective and low-cost.

Acknowledgements

The authors would like to acknowledge the financial support of this work from National Natural Science Foundation of China (No. 21076174) and Zhangzhou Normal University (No. 2003 L20926). The authors also thank the anonymous referees for comments on this manuscript.

References

[1] Q. Li, J.P. Zhai, W.Y. Zhang, et al., Kinetic studies of adsorption of Pb(II), Cr(III) and Cu(II) from aqueous solution by sawdust and modified peanut husk, J. Hazard. Mater. 141 (2007) 163–167.
[2] J. Romero-Gonzĭalez, J.C. Walton, J.R. Peralta-Videa, et al., Modeling the adsorption of Cr(III) from aqueous solution onto Agave lechuguilla biomass: Study of the advective and dispersive transport, J. Hazard. Mater. 161 (2009) 360–365.
[3] X. Huang, X.P. Liao, B. Shi, Tannin-immobilized mesoporous silica bead (BT-SiO2) as an effective adsorbent of Cr(III) in aqueous solutions, J. Hazard. Mater. 173 (2010) 33–39.
[4] A. Lodi, D. Soletto, C. Solisio, A. Converti, Chromium(III) removal by Spirulina platensis biomass, Chem. Eng. J. 136 (2008) 151–155.
[5] F. Gode, E. Pehlivan, Removal of chromium(III) from aqueous solutions using LewatitS 100: the effect of pH, time, metal concentration and temperature, J. Hazard. Mater. 136 (2006) 330–337.
[6] M. Yigitoglu, M. Arslan, Selective removal of Cr(VI) ions from aqueous solutions including Cr(VI), Cu(II) and Cd(II) ions by 4-vinly pyridine/2-hydroxyethylmethacrylate monomer mixture grafted poly-(ethylene terephthalate) fiber, J. Hazard. Mater. 166 (2009) 435–444.
[7] S.S. Barala, N. Das, G.R. Chaudhury, S.N. Das, A preliminary study on the adsorptive removal of Cr(VI) using seaweed, Hydrilla verticillata, J. Hazard. Mater. 171 (2009) 358–369.
[8] P. Miretzky, A.F. Cirelli, Cr (VI) and Cr (III) removal from aqueous solution by raw and modified lignocellulosic materials, a review, J. Hazard. Mater. (2008), doi:10.1016/j.jhazmat.2010.04.060.

[9] Y.B. Zeng, H. Woo, G.H. Lee, J.B. Park, Adsorption of Cr(VI) on hexadecylpyridinium bromide (HDPB) modified natural zeolites, Micropor. Mesopor. Mater. 130 (2010) 83–91.
[10] F. Venditti, F. Cuomo, F. Lopez, et al., Effects of sulfate ions and slightly acidic pH conditions on Cr(VI) adsorption onto silica gelatin composite, J. Hazard. Mater. 173 (2010) 552–557.
[11] P.K. Ghosh, Hexavalent chromium [Cr(VI)] removal by acid modified waste activated carbons, J. Hazard. Mater. 171 (2009) 116–122.
[12] Y.H. Liu, L. Guo, J. Chen, Removal of Cr(III, VI) by quaternary ammonium and quaternary phosphonium ionic liquids functionalized silica materials, Chem. Eng. J. 158 (2010) 108–114.
[13] G.L. Huang, J.X. Shi, T.A.G. Langrish, Removal of Cr(VI) from aqueous solution using activated carbon modified with nitric acid, Chem. Eng. J. 152 (2009) 434–439.
[14] Y.T. He, S.J. Traina, Cr(VI) reduction and immobilization by magnetite under alkaline pH conditions: the role of passivation, Environ. Sci. Technol. 39 (2005) 4499–4504.
[15] F.J. Alguacil, M. Alonso, F. Lopez, A.L. Delgado, Uphill permeation of Cr(VI) Using Hostarex A327 as ionophore by membrane-solvent extraction processing, Chemosphere 72 (2008) 684–689.
[16] K.Y. Wang, T.S. Chung, Fabrication of polybenzimidazole (PBI) nanofiltration hollow fiber membranes for removal of chromate, J. Membr. Sci. 281 (2006) 307–315.
[17] M.M. Nasef, A.H. Yahaya, Adsorption of some heavy metal ions from aqueous solutions on Nafion 117 membrane, Desalination 249 (2009) 677–681.
[18] N.T. Hoai, D.K. Yoo, D. Kim, Batch and column separation characteristics of copper-imprinted porous polymer micro-beads synthesized by a direct imprinting method, J. Hazard. Mater. 173 (2010) 462–467.
[19] I. Dakova, I. Karadjova, I. Ivanov, et al., Solid phase selective separation and preconcetration of Cu(II) by Cu(II)-imprinted polymethacrylic microbeads, Anal. Chim. Acta 584 (2007) 196–203.
[20] F.Q. An, B.J. Gao, Adsorption characteristics of Cr(III) ionic imprinting polyamine on silica gel surface, Desalination 249 (2009) 1390–1396.
[21] M.N. Mohamad Ibrahim, C.S. Sipaut, N.N. Mohamad Yusof, Purification of vanillin by a molecular imprinting polymer technique, Sep. Purif. Technol. 66 (2009) 450–456.
[22] X.J. Wang, Z.L. Xu, J.L. Feng, et al., Molecularly imprinted membranes for the recognition of lovastatin acid in aqueous medium by a template analogue imprinting strategy, J. Membr. Sci. 313 (2008) 97–105.
[23] Z.F. Cai, H.J. Dai, S.H. Si, F.L. Ren, Molecular imprinting and adsorption of metallothionein on nanocrystalline titania membranes, Appl. Surf. Sci. 254 (2008) 4457–4461.
[24] L.C.S. Chou, C.C. Liu, Development of a molecular imprinting thick film electrochemical sensor for cholesterol detection, Sens. Actuators B 110 (2005) 204–208.
[25] M.X. Loukidou, A.I. Zouboulis, T.D. Karapantsios, K.A. Matis, Equilibrium and kinetic modeling of chromium(VI) biosorption by Aeromonas caviae, Colloids Surf. A: Physicochem. Eng. Aspects 242 (2004) 93–104.
[26] B. Preetha, T. Viruthagiri, Batch and continuous bisorption of chromium(VI) by Rhizopuc arrhizus, Sep. Purif. Technol. 57 (2007) 126–133.
[27] P. Agrawal, R. Patil, N. Kalyaneb, U.V.A. Joshi, Formulation and in-vitro evaluation of Zidovudine loaded calcium alginate microparticles containing copolymer, J. Pharm. Res. 3 (2010) 486–490.
[28] A.D. Eaton, L.S. Clesceri, A.E. Greenberg, Standard Methods for the Examination of Water and Wastewater, 20th ed., American Public Health Association, Washington, DC, 1999.
[29] M. Rafatullah, O. Sulaiman, R. Hashima, A. Ahmad, Adsorption of copper (II), chromium (III), nickel (II) and lead(II) ions from aqueous solutions by meranti sawdust, J. Hazard. Mater. 170 (2009) 969–977.
[30] T.S. Anirudhan, P.G. Radhakrishnan, Chromium (III) removal from water and wastewater using a carboxylate-functionalized cation exchanger prepared from a lignocellulosic residue, J. Colloid Interf. Sci. 316 (2007) 268–276.
[31] P. Lodeiro, A. Fuentes, R. Herrero, M.E. Sastre de Vicente, Cr (III) binding by surface polymers in natural biomass: the role of carboxylic groups, Environ. Chem. 5 (2008) 355–365.
[32] P. Miretzky, A. Fernandez Cirelli, Cr(VI) and Cr(III) removal from aqueous solution by raw and modified lignocellulosic materials: a review, J. Hazard. Mater. 180 (2010) 1–19.
[33] M. Aoyama, M. Kishino, T.S. Jo, Biosorption of Cr (VI) on Japanese Cedar Bark, Sep. Sci. Technol. 39 (2005) 1149–1162.
[34] P.A. Kumar, M. Ray, S. Chakraborty, Adsorption behaviour of trivalent chromium on amine-based polymer aniline formaldehyde condensate, Chem. Eng. J. 149 (2009) 340–347.
[35] M. Hamdi Karaoğlu, S. Zor, M. Uğurlu, Biosorption of Cr(III) from solutions using vineyard pruning waste, Chem. Eng. J. 159 (2010) 98–106.
[36] R. Elangovan, L. Philip, K. Chandraraj, Biosorption of hexavalent and trivalent chromium by palm flower (Borassus aethiopum), Chem. Eng. J. 141 (2008) 99–111.
[37] A.P.S. Batista, L.P.C. Romão, M.L.P.M. Arguelho, et al., Biosorption of Cr(III) using in natural and chemically treated tropical peats, J. Hazard. Mater. 163 (2009) 517–523.
[38] A.A. El-Bayaa, N.A. Badawy, E. Abd AlKhalik, Effect of ionic strength on the adsorption of copper and chromium ions by vermiculite pure clay mineral, J. Hazard. Mater. 170 (2009) 1204–1209.
[39] M.E. Mahmouda, O.F. Hafez, M.M. Osman, et al., Hybrid inorganic/organic alumina adsorbents -functionalized-purpurogallin for removal and preconcentration of Cr(III), Fe(III), Cu(II), Cd(II) and Pb(II) from underground water, J. Hazard. Mater. 176 (2010) 906–912.
[40] J. Anwar, U. Shafique, J.M. Anzano, et al., Removal of chromium (III) by using coal as adsorbent, J. Hazard. Mater. 171 (2009) 797–801.
[41] L. Monser, N. Adhoum, Tartrazine modified activated carbon for the removal of Pb(II), Cd(II) and Cr(III), J. Hazard. Mater. 161 (2009) 263–269.
[42] X.P. Huang, X.J. Chang, Q. He, et al., Tris(2-aminoethyl) amine functionalized silica gel for solid-phase extraction and preconcentration of Cr(III), Cd(II) and Pb(II) from waters, J. Hazard. Mater. 157 (2008) 154–160.
[43] Y. Wu, S.Z. Zhang, X.Y. Guo, H.L. Huang, Adsorption of chromium(III) on lignin, Bioresour. Technol. 99 (2008) 7709–7715.
[44] D. Mohan, K.P. Singh, V.P. Singh, Trivalent chromium removal from wastewater using low cost activated carbon derived from agricultural waste material and activated carbon fabric cloth, J. Hazard. Mater. 135 (2006) 280–295.